JBC Papers in Press. Published on August 14, 2019 as Manuscript RA119.008484
The latest version is at http://www.jbc.org/cgi/doi/10.1074/jbc.RA119.008484

The steroid hormone 20-hydroxyecdysone induces phosphorylation and aggregation of stromal interacting molecule 1 for store-operated calcium entry

Cai-Hua Chen[1,2], Yu-Qin Di[1], Qin-Yong Shen[1], Jin-Xing Wang[1], Xiao-Fan Zhao[1*]

1. Shandong Provincial Key Laboratory of Animal Cells and Developmental Biology, School of Life Sciences, Shandong University, Qingdao, 266237, China
2. Department of Entomology, College of Plant Protection, Northwest A & F University, Yangling, 712100, China

Running title: 20E promotes SOCE via GPCRs

[*]Corresponding author: Xiao-Fan Zhao. E-mail: xfzhao@sdu.edu.cn. GenBank number of STIM1: MK910371

Keywords: 20-hydroxyecdysone, stromal interacting molecule 1 (STIM1), phosphorylation, store-operated calcium entry (SOCE), cell signaling, insect development, hormone signaling, apoptosis

Abstract

Oligomerization of stromal interacting molecule 1 (STIM1) promotes store-operated calcium entry (SOCE); however, the mechanism of STIM1 aggregation is unclear. Here, using the lepidopteran insect and agricultural pest cotton bollworm (*Helicoverpa armigera*) as a model and immunoblotting, RT-qPCR, RNAi, and ChIP assays, we found that the steroid hormone 20-hydroxyecdysone (20E) upregulates STIM1 expression via G protein–coupled receptors (GPCRs) and the 20E nuclear receptor (EcRB1). We also identified an ecdysone-response element (EcRE) in the 5'-upstream region of the *STIM1* gene and also noted that STIM1 is located in the larval midgut during metamorphosis. *STIM1* knockdown in larvae delayed pupation time, prevented midgut remodeling, and decreased 20E-induced gene transcription. *STIM1* knockdown in a *H. armigera* epidermal cell line, HaEpi, repressed 20E-induced calcium ion influx and apoptosis. Moreover, 20E induced STIM1 clustering to puncta and translocation toward the cell membrane. Inhibitors of GPCRs, phospholipase C (PLC), and inositol trisphosphate receptor (IP3R) repressed 20E-induced STIM1 phosphorylation, and we found that two GPCRs are involved in 20E-induced STIM1 phosphorylation. 20E induced STIM1 phosphorylation on Ser-485 through protein kinase C (PKC), and we observed that Ser-485 phosphorylation is critical for STIM1 clustering, interaction with calcium release-activated calcium channel modulator 1 (Orai1), calcium ion influx, and 20E-induced apoptosis. These results suggest that 20E upregulates STIM1 phosphorylation for aggregation via GPCRs, followed by interaction with Orai1 to induce SOCE, thereby promoting apoptosis in the midgut during insect metamorphosis.

Introduction

Cytosolic calcium, a key secondary signaling messenger in almost every cell, regulates a wide range of biological processes (1), such exocytosis, cell proliferation, and apoptosis (2). However, the concentration of cytosolic Ca^{2+} is well controlled at a low concentration (~nM) compared with that in the extracellular environment (~mM) by storing Ca^{2+} in the intracellular calcium store of endoplasmic reticulum (ER), or excluding Ca^{2+} outside cells, because it binds water less tightly and precipitates phosphate (3). The cytosolic

Ca^{2+} concentration can be increased for signaling by the depletion of intracellular Ca^{2+} store that triggers Ca^{2+} influx into cells from the outside environment. This kind of Ca^{2+}-entrance is called store-operated Ca^{2+} entry (SOCE) (4), and the channel is called the intracellular store-operated Ca^{2+} channel (SOC) or Ca^{2+} release-activated channel (CRAC) (5).

Stromal interacting molecule (STIM1), as an intracellular calcium sensor locates on the ER, is essential for SOCE (6,7). The N-terminus of STIM1 is inside the ER lumen and C-terminus lies outside the ER (8). When ligands bind to cell membrane receptors, such as G protein-coupled receptors (GPCRs), phospholipase C (PLC) is activated by G protein alpha (Gα) to produce IP_3 (inositol 1,4,5-trisphosphate). IP_3 binds with its intracellular receptor (IP_3R) to release cell-stored Ca^{2+} from the ER into the cytosol (9). The depletion of cell-stored Ca^{2+} stimulates STIM1 aggregates to form oligomers via EF-hand and sterile alpha-motif domain (EF-SAM) (10). Ca^{2+} dissociation determines a switch of the conformation of the luminal domain (11). After rapid oligomerization, STIM1 oligomers translocate to the ER-PM (ER-plasma membrane) junctions (12). The proximity between the ER membrane and the PM at ER-PM junctions means that the oligomers of STIM1 directly interact with the calcium release-activated calcium channel modulator (Orai) on the PM to induce Ca^{2+} entry (13). Orai is the essential protein that participates in SOCE (14) (15). Orai1 assembles as a hexamer upon stimulation by agonists to bind with STIM1 oligomers to allow Ca^{2+} entry in *Drosophila* (16) and humans (17). Oligomerization of STIM1 promotes SOCE in humans; however, the upstream regulator of STIM1 aggregation and the outcome are unclear.

Phosphorylation as a post-translational modification plays an important role in protein functions. Various phosphorylation sites of STIM1 have been detected in mammals (18), and the outcomes of different STIM1 phosphorylations are different in various cellular processes. For examples, estrogen inhibits oligomerization and Ser575 phosphorylation of STIM1 to reduce SOCE in human bronchial epithelial cells (19). Phosphorylation of STIM1 on Ser486 and Ser668 during mitosis in HEK293 cells represses SOCE (20). The phosphorylation of STIM1 on Ser575, Ser608, and Ser621 is required for SOCE in HEK293 cells (21). However, the phosphorylation and mechanism of STIM1 in insect are unclear.

Steroid hormones, such as mammal estrogen and insect molting hormone 20-hydroxyecdysone (20E), are small fat-soluble molecules. They can diffuse into cells through the PM and bind with estrogen receptors in mammals (22), and the nuclear receptor 20E nuclear receptor (EcRB1) in insects (23), to regulate gene expression for animal development. In recent years, studies have shown that estrogen induces rapid cellular responses, such as rapid calcium increase, via GPCRs (24). 20E also induces Ca^{2+} increase via GPCRs in *Bombyx mori* (25) and in *Helicoverpa armigera* (26). Such a rapid signal pathway acting before gene transcription is called a nongenomic pathway. In *H. armigera*, ecdysone-responsive GPCRs, ErGPCR-1 (26) and ErGPCR-2 (27) on the cell membrane, have been identified to participate in the 20E-nongenomic pathway by inducing rapid calcium entry, and protein phosphorylation in transcription complexes for gene transcription during insect development (28,29). Dependent on the increased-intracellular Ca^{2+} levels, 20E causes a switch from autophagy to apoptosis in the midgut of *H. armigera* during metamorphosis (30). Ca^{2+}/calmodulin-dependent protein kinase II (CaMKII) is activated by Ca^{2+} to regulate transcription factor ultraspiracle (USP1) acetylation for gene expression (31). 20E, via GPCRs, induces Ca^{2+} influx through the Orai1 channel in *H. armigera* (32); however, currently available data are insufficient to determine the mechanism of steroid hormone-induced Ca^{2+} entry , without

understanding the role of the key initiator STIM1 in the process. The 20E is also produced by various plants, such as *Cyanotis vaga*, to disrupt development of insect pests (33), however, the mechanism of is unclear.

To address these questions, the present study focused on STIM1 using the agricultural pest, cotton bollworm (Lepidoptera *H. armigera*), as a model. We revealed that 20E, via GPCRs and EcRB1, upregulated STIM1 expression. 20E, via GPCR-, PLC-, IP_3R- and PKC-signaling, induced the phosphorylation of STIM1 at Ser485, which was essential for aggregation of STIM1 and calcium influx leading to apoptosis. STIM1 is essential for the degradation of the larval midgut and 20E-regulated gene expression. Our study proved that 20E induces SOCE via a GPCR-mediated nongenomic pathway to induce insect metamorphosis.

Results

STIM1 was upregulated and exists in a phosphorylated form during metamorphosis

We prepared rabbit-derived polyclonal antibodies against the STIM1 and examined their specificity by western blot. We found that the anti-serum had ability to recognize a 65-kDa molecular weight (MW) protein specifically, which was consistent with the predicted MW of STIM1. However, the pre-serum of rabbit did not recognize any protein (Fig. 1A), which suggested that the antibodies had specificity to STIM1 of *H. armigera*. The expression pattern of STIM1 in certain tissues from 5th instar larvae to the pupal stage was detected using western blotting to verify the involvement of STIM1 in larval development and metamorphosis. STIM1 was detected in the epidermis, midgut, and fat body, with a marked increase in its level at the metamorphic stage from 6th instar larvae to the late pupae (Fig. 1B). The data were quantified based on three independent experiments (Fig. 1C). The MW of STIM1 was decreased by treatment with λPPase, suggesting that STIM1 was phosphorylated posttranslationally (Fig. 1D). These data suggested that STIM1 plays an important role in insect metamorphosis.

20E upregulates STIM1 expression through a membrane receptor and a nuclear receptor

The increased expression level of STIM1 suggested that 20E might upregulate STIM1 expression, because the 20E titer increases during metamorphosis in lepidopteran insects (34). To verify the upregulation of STIM1 by 20E, we examined the level of STIM1 in the midgut using western blotting after 20E-injection into larvae. The results showed that the level of STIM1 was increased by 20E injection in a time and concentration-dependent manner (Figs. 2A and B). Quantitative analysis confirmed that the expression of STIM1 was increased by 20E induction significantly (Figs. 2C and D). The results demonstrated that 20E increased the expression level of STIM1 in the midgut.

GPCRs, such as ErGPCR-1 (26) and ErGPCR-2 (27), transmit 20E signals in the cell membrane to promote the formation of the EcRB1/USP1 complex for gene transcription (29,35). Therefore, we knockdown the expression of *ErGPCR-1*, *ErGPCR-2*, *EcRB1*, and *USP1*, respectively, in HaEpi cells and detected *STIM1* expression to address the signaling axis of 20E upregulated STIM1 expression. The qRT-PCR results showed that the 20E-promoted expression of *STIM1* was repressed after knockdown of *ErGPCR-1*, *ErGPCR-2*, *EcRB1*, and *USP1* (Fig. 3A-D). The interference efficiencies were detected after transfection of dsRNA alone (Fig.3E). The results suggested that 20E, via the ErGPCR-1 and ErGPCR-2 cell membrane GPCRs and EcRB1/USP1 nuclear receptor transcription complex signaling axis, upregulates *STIM1* expression.

To confirm the above hypothesis, the EcR binding element (EcRE) was analyzed and an EcRE was predicted in the 5'-upstream genomic DNA sequence of *STIM1* in the genome of *H. armigera* using the JASPAR website (http://jaspar.genereg.net/). We identified an EcRE in the promoter region of STIM1,

5'-GCGGTTAATGCATTA-3', which is very similar to the previously identified EcRE, 5'-GGGGTCAATGAACTG-3', in the promoter region of HR3 (28) with a few base differences (Fig. 3F). ChIP experimental analysis proved that EcRB1 could bind to the EcRE in the promoter region of *STIM1* (Fig. 3G). These results showed that the different base had no effect on the binding of EcRB1 and EcRE. This data indicated that 20E directly promotes *STIM1* transcription by EcRB1 binding to the EcRE.

STIM1 is located in the larval midgut during metamorphosis

To identify the function of STIM1 in the larval midgut, we first examined the localization of STIM1 in the midgut. STIM1 was subjected to immunohistochemistry using polyclonal antibodies. We found that little STIM1 distributed in the midgut of sixth instar larvae at 24 h. In contrast, abundant STIM1 was detected in the midgut of sixth instar larvae at 48 h and at 96 h. In addition, STIM1 was mainly located in the larval midgut, with little STIM1 signal in the imaginal midgut during metamorphosis (Fig. 4). These results suggested that STIM1 is expressed in the larval midgut, and might be related to midgut apoptosis during metamorphosis.

***STIM1* knockdown suppressed metamorphosis, midgut programmed cell death (PCD), and 20E-induced gene expression**

STIM1 was knocked down by injecting *dsSTIM1* into fifth instar larvae and sixth instar larvae to explore the function of STIM1 during insect metamorphosis. Compared with that in the *dsGFP* injection control group, pupation was delayed by about 30 hours in the *dsSTIM1* injection group (Figs. 5A and B). The efficiency of RNA interference of *STIM1* was confirmed by western blotting (Fig. 5C). In *H. amigera*, the midgut turns red at 72 h of the sixth instar larvae when it occurs apoptosis during metamorphosis (36, 37) However, the midgut did not turn red after injection of *dsSTIM1* for 96 h and the larval midgut did not separate from imaginal midgut, compared with the larvae injected with the control *dsGFP* injection (Figs. 5D and E). qRT-PCR analysis showed that the expression of 20E-response genes, *HR3*, *EcRB1*, *USP1*, and *BrZ7*, and apoptosis-related genes, *Caspase-3* and *Caspase-6*, were repressed in the midgut after interference by *dsSTIM1* in the larval midgut (Fig. 5F). Similar results were observed in HaEpi cells after knockdown of *STIM1* (Fig. 5G). These results demonstrated that STIM1 participates in the larval midgut PCD and metamorphosis.

To address the mechanism of STIM1's participation in 20E promoted gene expression and metamorphosis, the intracellular Ca^{2+} levels were examined after *STIM1* was knocked down in HaEpi cells. 20E promoted the release of intracellular-stored Ca^{2+} ions and thus caused Ca^{2+} influx (Fig. 6A). However, the release of intracellular Ca^{2+} was unaffected, but the influx of extracellular Ca^{2+} was repressed (Fig. 6B) when *STIM1* was knocked down. Besides, 20E-induced apoptosis also was detected using TUNEL assay after knockdown of *STIM1*. 5 μM 20E induced apoptosis in 72 h in the blank control and *dsGFP* control. However, the apoptosis was repressed after knockdown of *STIM1* (Fig. 6C). The statistical analysis of the ratio of apoptotic cells showed similar results (Fig. 6D). The efficacy of *STIM1* knockdown by RNAi was confirmed using qRT-PCR (Fig. 6E). These data suggested that STIM1 participates in 20E-promoted SOCE, which is necessary for 20E pathway gene expression and apoptosis.

20E induced STIM1 aggregation

To demonstrate the mechanism of STIM1's function in 20E-promoted SOCE, we examined the subcellular localization of STIM1 under regulation by 20E using overexpression of STIM1-GFP in HaEpi cells. Thapsigargin (Tg), as an agonist of SOC, triggers stored calcium release, but inhibits the calcium pump Sarcoplasmic/Endoplasmic Reticulum Ca^{2+}-ATPase (SERCA) on the ER will

suppress calcium back into the ER from the cytosol (38). Therefore, we used Tg as a positive control of calcium-store depletion. By staining the cell membrane with wheat germ agglutinin (WGA), we found that 20E promoted STIM1-GFP to form oligomers and move toward the PM, where they were located underneath the PM. The aggregation of STIM1-GFP disappeared after the addition of calcium into DPBS followed by 20E treatment that refilled the intracellular calcium store. Tg promoted similar aggregation and subcellular translocation of STIM1-GFP to 20E; however, the addition of calcium did not eliminate the Tg-induced aggregation of STIM1-GFP because Tg blocked the refill of the calcium store (Fig. 7A). The percent of STIM1-aggregated cells were calculated and suggested the same results (Fig. 7B). The overexpressed STIM1-GFP and GFP tag protein were detected by western blotting (Fig. 7C). These data suggested that 20E induces STIM1 aggregation and cell membrane translocation upon depletion of stored calcium.

20E induced STIM1 phosphorylation via GPCRs

Considering STIM1 was phosphorylated in larvae, the pathway by which 20E might stimulate STIM1 phosphorylation was analyzed using various inhibitors and knockdown of *GPCRs*. There was no effect on the molecular sizes of the overexpressed GFP-tag control (Fig. 8A a). However, the overexpressed STIM1-GFP appeared an upper band under 20E regulation in Ca^{2+} free condition. Moreover, the amount of the upper band was reduced by the addition of calcium and eliminated by λPPase treatment (Fig. 8A b), suggesting that 20E induced STIM1 phosphorylation under condition of calcium shortage. The GPCR and ryanodine receptor (RYR) inhibitor Suramin (39), the PLC inhibitor U73122 (40), the IP_3R inhibitor Xestospongin C (XeC) (41), and the PKC inhibitor chelerythrine chloride (CC) (42) all repressed 20E-induced STIM1 phosphorylation (Fig. 8B). Moreover, knockdown of *ErGPCR-1* and *ErGPCR-2* using RNAi inhibited 20E-induced phosphorylation of STIM1 (Fig. 8C). The efficacies of knockdown of *ErGPCR-1* and *ErGPCR-2* were confirmed using qRT-PCR (Figs. 8D and E). These results suggested that 20E promotes STIM1 phosphorylation through the GPCR-, PLC-, IP_3R-, and PKC-signaling axis.

In addition, anti-pSer, anti-pThr, and anti-pTyr antibodies were used to detect the type of STIM1 phosphorylation in the epidermis and midgut. The anti-pSer antibody detected a band from the purified STIM1. However, the anti-pThr and anti-pTyr antibodies did not detect a band (Fig. 8F), which suggested that STIM1 phosphorylation occurred on serine residues.

Phosphorylation of STIM1 was required for STIM1 aggregation and calcium influx

The phosphorylation site of STIM1 was identified to confirm the outcome of phosphorylation of STIM1. STIM1 phosphorylation was serine-phosphorylation and was regulated by PKC (as confirmed by the inhibitor experiments and antibodies detection); therefore, we predicted the PKC-phosphorylation sites. Three PKC-type serine phosphorylation sites, Ser360, Ser395, and Ser485, were predicted using NetPhos (www.cbs.dtu.dk/services/NetPhos/). We constructed three mutant plasmids in which the possible phosphorylated serines were replaced by alanine (S360A, S395A, and S485A) and overexpressed the mutant proteins in HaEpi cells. The phosphorylation of STIM-GFP wild-type and mutants were detected by western blotting under 20E or DMSO treatment. Under 20E induction, the upper band was detected in the wild-type, Ser360 mutant, and Ser395 mutant, but not in the S485A mutant, compared with that in the DMSO control (Fig. 9A), which suggested that 20E induced STIM1 phosphorylation at Ser485.

To explore the outcomes of STIM1 phosphorylation, STIM1-GFP and the STIM1-S485A-GFP mutant were overexpressed in HaEpi cells and various cellular processes were examined. The

results showed that the STIM1-S485A-GFP mutant could not aggregate under 20E induction in HaEpi cells compared with that in STIM1-GFP overexpressing cells (Fig. 9B and C). In addition, DMSO, as a solvent control, did not induce Ca^{2+} release or influx in GFP and STIM1-GFP overexpressing cells. In contrast, 20E induced normal Ca^{2+} release in GFP, STIM1-GFP and STIM1-S485A-GFP mutant overexpressing cells; however, 20E triggered much more Ca^{2+} influx in STIM1-GFP overexpressing cells than that in GFP or STIM1-S485A-GFP mutant overexpressing cells (Fig. 9D), which suggested that S485 was critical for the function of STIM1 in calcium entry. Co-immunoprecipitation (Co-IP) using antibodies against GFP detected STIM1-GFP and Orai1-RFP together under 20E induction, but did not detect STIM1-S485A-GFP and Orai1-RFP together under 20E induction (Fig. 9E), which suggested that the interaction between STIM1 and Orai1 relies on phosphorylation of S485 in STIM1.

High levels of 20E induce intracellular calcium increase for apoptosis (43). To determine the effect of STIM1 phosphorylation on 20-induced apoptosis, we overexpressed the STIM1-GFP and mutation type STIM1-S485A-GFP. Apoptosis by TUNEL assay should the overexpression of the STIM1-GFP increased apoptosis under 5 μM 20E induction for 48 h. However, the overexpression of the mutant STIM1-S485A-GFP did not increase the apoptosis under same condition (Fig. 10A and B). These results suggested that the phosphorylation-S485 of STIM1 is required for 20E-induced apoptosis.

Discussion

20E can induce Ca^{2+} entry; however, the mechanism is unclear. In the present study, we demonstrated that 20E, via cell membrane receptor GPCRs and the ecdysone nuclear receptor EcRB1, induced STIM1 expression for Ca^{2+} influx. 20E induced STIM1 phosphorylation at Ser485 through the GPCR-, PLC-, IP_3R- and PKC-signaling axis to promote STIM1 aggregation, interaction with Orai1 for Ca^{2+} entry, and finally, apoptosis. Therefore, 20E via STIM1 induces SOCE for apoptosis in the midgut during metamorphosis.

20E upregulates STIM1 expression through GPCRs and nuclear receptor EcRB1

STIM1 is a Ca^{2+} sensor in cells that initiates Ca^{2+} entry when the cellular Ca^{2+} store is depleted (44). STIM1 is expressed in a range of human cells and tumor cells to suppress growth (18). The expression of STIM1 can be positively or negatively regulated by androgens (45), nuclear factor kappa B (NF-κB) (46), and glucocorticoid inducible kinase 1 (SGK1) (47). In the present study, we found that steroid hormone 20E upregulates STIM1 expression through GPCRs and the 20E nuclear receptor, EcRB1. This is the first report that GPCRs participate in the expression of STIM1which was induced by steroid hormone.

20E has a high titer during insect metamorphosis (34) and regulates gene transcription through genomic (23) and nongenomic pathways (25). Studies have shown that 20E via the nongenomic pathway directs the genomic pathway for gene expression (29,48). ErGPCR-1 and ErGPCR-2 transmit the 20E signal by the nongenomic pathway and finally regulate gene expression via the EcRB1/USP1-mediated genomic pathway for apoptosis in the midgut during metamorphosis in *H. armigera* (26,27). In the present study, we demonstrated that membrane receptors ErGPCR-1 and ErGPCR-2 are critical for the expression of STIM1 which was upregulated by 20E in the larval midgut. The results further verified that 20E regulates gene expression through the nongenomic pathway.

We found the nuclear receptor EcRB1 is also necessary for 20E-induced STIM1 expression. To date, most genes in the 20E pathway have been found to be upregulated by 20E via the EcRB1/USP1 transcription complex binding to EcRE, for example *HR3* (49). The EcRE1 in the *MHR3* promoter region of *Manduca sexta* (50)

5'-GGGGTCAATGAACCG-3' is highly conserved with the EcRE in the *HHR3* promoter region of *H. armigera* 5'-GGGGTCAATGAACTG-3' (29). In the present study, we identified an EcRE in the promoter region of *STIM1*, 5'-GCGGTTAATGCATTA-3', which is very similar to the EcRE in the *HHR3* promoter. All these EcREs have a conservative core sequence 5'-^{7}AATG^{10}-3'. The EcRE of STIM1 also has the core site, so it may be a canonical binding site for EcR. In addition, an EcRE was predicted in the promoter region of *STIM1* from *B. mori*, *D. melanogaster*, *Plutella xylostella*, and *Apis florea*. The sequences of the EcRE only have one base difference between *H. armigera* and *B. mori* (Table 1). These data indicated that the EcRE in the promoter region of *STIM1* is widespread in insects.

20E promotes STIM1 phosphorylation and aggregation for SOCE via the nongenomic pathway

20E regulates insect metamorphosis not only by transcriptional mechanisms, but also by posttranslational mechanisms, such as protein phosphorylation. Protein phosphorylation of calponin (51), CDK10 (28), USP1 (29), and EcRB1 (35) is involved in the 20E signal transduction pathway. Our results revealed that via GPCR-, PLC-, and IP_3R- signaling, 20E induces intracellular Ca^{2+} release from the ER. GPCR-triggered intracellular Ca^{2+} release binds to and activates PKC in humans (3). Our results showed 20E increases Ca^{2+} and promotes PKC-phosphorylation of STIM1 on Ser485 via GPCRs.

It is known that Ca^{2+} depletion inside ER lumen induces STIM1 aggregation (52), The function of STIM1 phosphorylation is different in various cellular processes, based on the phosphorylation sites (19). In the present study, we demonstrated that 20E induces phosphorylation of STIM1 at Ser485, which is critical for STIM1 aggregation and the subsequent interaction with the Orai1 channel to trigger SOCE. The phosphorylation of STIM1 at Ser485 relies on Ca^{2+} release from the ER, because the IP_3R inhibitor XeC can repress STIM1 phosphorylation (Figure 8B), which explains the gapped mechanism between the Ca^{2+} depletion inside ER lumen and STIM1 aggregation in cytosol.

20E induced SOCE for midgut apoptosis via STIM1

The increased intracellular Ca^{2+} induced by steroids has multiple functions. In hepatocytes, the intracellular Ca^{2+} level is increased by estrogen to induce ERK activation for growth (53). In *Drosophila*, the expression of STIM1 in embryonic and larval tissues regulates growth and patterning of imaginal discs (54). In *B. mori*, 20E mediates PCD through the Ca^{2+}-PKC-caspase-3 pathway (25). In *H. armigera*, 20E triggers extracellular Ca^{2+} influx into cells through the nongenomic pathway to promote autophagy and the switch from autophagy to apoptosis (30). The increased Ca^{2+} triggers 20E-response gene transcription and apoptosis by mediating the formation of EcRB1/USP1 transcriptional complexes and binding to EcRE (29). Ca^{2+} induction of apoptosis is dependent on the Ca^{2+} concentration (43). In the present study, we confirmed that 20E induces Ca^{2+} influx via SOCE for apoptosis in the midgut during metamorphosis in *H. armigera*. We also observed an increase in STIM1 levels in the epidermis and fat body. Orai1 was also observed to increase in the epidermis and fat body in *H. armigera* (32). However, the epidermis and fat body do not undergo apoptosis during metamorphosis. Thus, the mechanism needs to be further clarified in a future study.

Conclusion

20E induced Ca^{2+} release and STIM1 phosphorylation at Ser485 through the GPCRs-, PLC-, IP_3R-, and PKC- signaling axis, which caused STIM1 aggregation. Aggregated-STIM1 moves toward the ER-PM junction and interacts with Orai1 on the PM for Ca^{2+} entry. Then, EcRB1 binds to EcRE to upregulate the transcription of *STIM1* and other 20E pathway genes in a positive feedback manner. Thus, 20E

induces apoptosis in the midgut during metamorphosis via SOCE (Fig. 11).

Materials and methods

Insects and HaEpi cells

Cotton bollworms, *Helicoverpa armigera*, were cultured in our laboratory at 27 ± 1 °C with a photoperiod of 14 h light/10 h dark. The larvae were reared on an previously described artificial diet (55). The HaEpi cell line was derived from the epidermis of *H. armigera* in our laboratory (56) and has been used for research of hormone regulation, RNA interference (RNAi), and overexpression of proteins (29,35). The HaEpi cells at 50 passages without mycoplasma contamination were cultured in Grace's medium with 10% fetal bovine serum (FBS) (Biological Industries, Beit-Haemek, Israel) at 27 °C for experiments.

The antibodies for experiments

A fragment of *STIM1* (encoding amino acids 1–208) was expressed in *Escherichia coli* Rosetta, to be used as antigen. Rabbit polyclonal antibodies recognizing STIM1 were prepared in our laboratory according to a previously reported method (57). Rabbit polyclonal antibodies against β-actin and other monoclonal tag antibodies, such as anti-GFP, and anti-RFP from mouse, were purchased from ABclonal Company (Wuhan, China).

Protein extraction and western blotting

The total protein of tissues was extracted using extraction buffer [40 mM Tris-HCl, 1 mM phenylmethanesulfonyl fluoride (PMSF), pH 7.5]. After grinding the tissue completely, the homogenate was centrifuged at 10,000 × *g* at 4 °C for 10 min. The supernatant was collected, and Bradford's method was used to determine the protein concentration (58). To extract proteins from HaEpi cells, the cells were collected and lysed using radio immunoprecipitation assay buffer (RIPA, 50 mM Tris-HCl, pH 7.4, 150 mM NaCl, 1 mM EDTA, 1% NP-40, 0.1% SDS) (Beyotime, Beijing, China) plus protease inhibitors (Yeasen, Shanghai, China). After the protein concentrations were detected, an appropriate amount of loading buffer was added to the lysate and then the samples were boiled for 10 min. For each sample, 50 μg of protein was subjected to sodium dodecyl sulfate polyacrylamide gel electrophoresis (SDS-PAGE). The proteins were transferred onto nitrocellulose membranes electrophoretically. Protein Ladder (Thermo Fisher Scientific, Vilnius, Lithuania) markers were used to identify the molecular weights of target proteins. The membranes were incubated at room temperature in blocking buffer [5% fat-free powdered milk in Tris-buffered saline (TBS, 10 mM Tris-HCl, 150 mM NaCl, pH 7.5)] for 1 h. Primary antibodies were diluted with blocking buffer and incubated with the membranes at 4 °C for overnight (anti-STIM1: 1:100; β-actin: 1:5000; anti-GFP, -RFP and -His: 1:5000). The membrane was washed three times with 1 × TBST (0.1% Tween-20 in 1 × TBS) for 10 min each time, and the corresponding second antibody conjugated to alkaline phosphatase (AP) (anti-rabbit or anti-mouse IgG (ZSGB-BIO, Beijing, China)) was diluted to 1:5,000 with the same blocking buffer. The protein signal was observed in 10 mL 1×TBS combined with 40 μL of 0.75% p-nitro-blue tetrazolium chloride (NBT) and 30 μL of 0.5% 5-bromo-4-chloro-3- indolyl phosphate (BCIP, Sangon, Shanghai, China) in the dark for 20 min.

λ-phosphatase (λPPase) treatment

Proteins were extracted from tissues or cells using RIPA buffer. Forty microliters of protein (2 mg/mL) was incubated with 0.5 μL of λ phosphatase (λPP), 5 μL of 10 × buffer, and 5 μL of $MnCl_2$ (10 mM) at 30 °C for 30 min, according to the manufacturer's specifications (New England Biolabs, Beijing, China). The proteins were subjected to SDS-PAGE using 7.5% low concentration gels for western blotting analysis. Protein phosphorylation was examined via variations in molecular mass. β-actin was detected as the protein quality control. Controls were performed by the same method without λPPase.

Hormonal regulation in larvae

20E was dissolved in dimethyl sulfoxide (DMSO) at a storage concentration of 20 mM (9.6 mg/mL). 20E was diluted to 10 ng/μL, 20 ng/μL, 40 ng/μL, and 100 ng/μL using sterile 1 × phosphate-buffered saline (PBS; 140 mM NaCl, 2.7 mM KCl, 10 mM Na_2HPO_4, 1.8 mM KH_2PO_4) and injected 5 μL into the 6 th-6 h larval hemocoel for 12 h. Similarly, 500 ng of 20E was injected into the larval hemocoel for different times (1, 3, 6, 12, and 24 h). The proteins were then extracted from the larval midguts. Western blotting was then used to analyze STIM1 expression. An equal amount of DMSO was used as the solvent control.

***dsRNA* synthesis**

RNAi primers with the T7 promoter (Table 2) were designed for PCR. About 500 bp of the target gene cDNA was used as the template to synthesize *dsRNA*. Both strands of the *dsRNA* were synthesized in one reaction according to the method described in the MEGAscript RNAi kit (Thermo Fisher Scientific, Waltham, MA, USA). The purity of *dsRNA* is critical for the efficacy of RNAi in larvae. We used the phenol-chloroform method to purify the *dsRNA* according to a previous study (35). Long *dsRNAs* suppress the expression of a target gene in worms specifically (59), which can be broken down into several smaller fragments of the *dsRNAs in vivo* for different mRNA targets (60). Long *dsRNAs* also work well in lepidopteran insects (61).

RNAi in HaEpi cells

HaEpi cells were cultured in Grace's medium with 10% fetal bovine serum (FBS) (Biological Industries, Beit-Haemek, Israel) at 27 ℃ to about 80% confluence in 6 well plates, and then 2 μg of *dsRNA* was transfected into the cells using the QuickShuttle-enhanced transfection reagent (Biodragon Immunotech, Beijing, China) in 2 mL Grace's medium with 10% FBS for 24 h. 20E (2 μM) or DMSO were then used treat cells for 12 h. Total RNA was isolated using TransZol (TransGen, Beijing, China) and reverse transcribed into single-stranded cDNA using 5 × All-In-One RT MasterMix (Applied Biological Materials, Vancouver, Canadian) for quantitative real-time PCR analysis. Control cells were prepared using the same amount of *dsGFP*.

RNAi in larvae

The *dsRNA* was diluted to the appropriate concentration with nuclease-free PBS. The sterile *dsRNA* was injected into the larval hemocoel twice after the larvae were immobilized on ice. The first injection was into 5th instar 12 h larvae (1 μg), and the second was into 6th instar 6 h larvae (2 μg). Each group contained 30 larvae and the experiments were repeated three times. Injection of *dsGFP* was used as the control. The detailed method was described previous (35).

Quantitative real-time reverse transcription polymerase chain reaction (qRT-PCR)

The corresponding primers were designed (Table 2) for qRT-PCR using the first strand cDNA as a template. The program was 95 °C 15 min; 95 °C 15 s, 60 °C 60 s, 78 °C reading plate 2 s; 40 cycles; 65 °C to 95 °C analysis dissolution curve, interval 0.5 ºC. After obtaining the cycle threshold (Ct) value, the relative mRNA expression levels were calculated using the formula $2^{-\Delta\Delta Ct}$ (62). $2^{-\Delta\Delta Ct}=2^{-[\Delta Ct\ \text{experimental group}\Delta Ct\ \text{control group}]}$, $\Delta Ct_{\text{experimental group}}$ indicates the difference between the Ct of the gene and the average Ct of the *ACTB* (β-actin) in the experimental group. The $\Delta Ct_{\text{control group}}$ indicates the difference between the Ct value of the gene and the average Ct of *ACTB* in the control group.

Chromatin immunoprecipitation (ChIP)

The EcRB binding element (EcRE) in the 5'-upstream genomic DNA sequence of *STIM1* in the genome of *H. armigera* was analyzed using the JASPAR website (http://jaspar.genereg.net/). HaEpi cells were transfected with pIEx-4-EcRB1-RFP-His plasmid for 72 h and then treated with 20E or DMSO for 3 h. After incubating at 37 °C for 10 minutes in 1% formaldehyde, 0.125 M glycine was then added at 25 °C for 10 min to terminate the cross-linking. The cells were washed twice with 1 × PBS and then

suspended in SDS lysis buffer. The DNA was broken into fragments of 200–1000 bp by sonication (250 W for 9 seconds, interval of 9 seconds, 10 times). After centrifugation, 30 μL Protein A were added to the supernatants and followed by centrifugation to clean the nonspecifically recognized proteins. The sample was divided into three equal parts. One part was used as the input control, one was incubated without antibodies as a control, and the last part was treated with anti-RFP antibodies to precipitate EcRB1-RFP and the EcRB1-RFP bound ecdysone response element (EcRE) fragments in the *H. armigera STIM1* promoter. Nonspecific IgG from mouse was used as a control. The EcRE fragments were purified using a ChIP Assay Kit (Beyotime) according to the manufacturer's instructions. The enrichment of EcRE fragments in different experiments was analyzed using qRT-PCR with ChIP assay primers (primer EcRE) (Table 2). Results were presented as percentage of enrichment of EcRE fragments in samples relative to the input (EcRE fragments in the sample before RFP antibody immunoprecipitation). % Input = (sample precipitated by RFP antibody - sample without antibody)/input × %.

Hematoxylin and eosin (HE) staining of tissues and immunohistochemistry

The larval midguts (6th-24 h, 6th-48 h, and 6th-96 h) were isolated, fixed with 4% paraformaldehyde at 4 °C overnight, and then dehydrated in a gradient ethanol series. The tissues were embedded in paraffin, sliced into 7-μm sections using a paraffin-slicing machine, and adhered to gelatin-coated glass slides. The slides were dried at 42 °C overnight and subsequently dewaxed, dehydrated in a gradient ethanol series. Hematoxylin and eosin were used to stain nuclei and cytoplasm following the method described in our previous work (63). For immunostaining, the tissue slices were blocked using 2% bovine serum albumin (BSA) for 1 h and then incubated with serum (pre-serum or anti-STIM1 serum: 1:50) overnight at 4 °C. The slides were then washed with 1×PBS three times. Goat anti-rabbit DyLight 488 secondary antibodies (Abbkine, Wuhan, China) were incubated with the slices for 3 h and then the slices were washed three times. Positive signals were observed using an Olympus BX51 fluorescence microscope (Shinjuku-ku, Tokyo, Japan).

Calcium ion detection in HaEpi cells

HaEpi cells were incubated in culture dishes with fresh Grace's medium with 10% FBS for 24 h and reached 80% confluence. AM ester Calcium Crimson™ dye (Invitrogen, Carlsbad, CA, USA) was added to the medium to final concentration 3 μM for 30 min at 27 °C. The cells were washed with Ca^{2+}-free 1× Dulbecco's phosphate-buffered saline (DPBS) (2.7 mM KCl, 1.5 mM KH_2PO_4, 138 mM NaCl and 8 mM Na_2HPO_4) three times and kept in 500 μL DPBS. The fluorescence of cells before any treatment was detected using a Zeiss LSM 700 laser confocal microscope (Carl Zeiss, Oberkochen, Germany) every 6 s for 60 s as background. Then, 500 μL of DPBS with 4 μM 20E or DMSO was added dropwise onto the plate over 60 s. Subsequently, 1 mL of DPBS with Ca^{2+} (1 mM) and 20E (2 μM) were added at 240 s. Each image's fluorescence intensity was collected for 420 s using the Image pro-plus software (Media Cybernetics, Rockville, MD, USA).

Overexpression of proteins

The pIEx-4-GFP/RFP-His vector that was fused with green (GFP) or red fluorescent protein (RFP) was used for the experiments in the insect cell line. The open reading frames (ORFs) of the target genes (*STIM1*, *ORAI1*, and *EcRB1*) were amplified using primers (Table 2) and inserted into the vector. Five micrograms of recombinant plasmids were transfected into HaEpi cells using the QuickShuttle-enhanced transfection reagent (Biodragon Immunotech). All the recombinant plasmids in the experiments contained a His tag. Cell fluorescence was observed using a Carl Zeiss LSM 700 laser scan confocal microscope (Thornwood, NY, USA).

Identification of the phosphorylation type of STIM1

The phosphorylation sites were predicted using NetPhos (www.cbs.dtu.dk/services/NetPhos/). The epidermis and midgut were isolated from 6th-72 h larvae. Total proteins were lysed using RIPA buffer and ground completely. STIM1 was isolated using immunoprecipitation with anti-STIM1 antibodies and detected by SDS-PAGE. The three anti-phosphorylation antibodies, a mouse monoclonal antibody (mAb) recognizing phosphoserine (Anti-pSer) (Abcam, Cambridge, UK, rabbit polyclonal antibodies (pAbs) recognizing phosphothreonine (Anti-pThr) (Immunechem, Burnaby, Canada), and a mouse mAb recognizing phosphotyrosine (Anti-pTyr) (Biodragon, Beijing, China), which were diluted by 1:100 with 2% BSA and used to detect the phosphorylation type of STIM1. Anti-mouse (AP) secondary antibodies (ZSGB-BIO, Beijing, China) were used to detect Anti-pSer and Anti-pTyr. Anti-rabbit (AP) secondary antibody (ZSGB-BIO, Beijing, China) was used to detect Anti-pThr.

Co-immunoprecipitation (Co-IP)

Plasmid constructs pIEx-4-STIM1-GFP-His or STIM1 mutant pIEx-4-STIM1-S485A-GFP-His and pIEx-4-Orai1-RFP-His were co-transfected into HaEpi cells for 72 h, respectively. The cells were washed with Ca^{2+}-free DPBS three times. The cells were then treated with 20E (2 μM in DPBS) for 30 min. The cells were lysed on ice for 30 min using RIPA buffer. The supernatant was collected through centrifugation at 12,000 × *g* for 10 min at 4 °C. The supernatant was added to protein A resin to eliminate non-specific binding and harvested by centrifugation (1,000 × *g* for 2 min). The lysate was incubated with anti-GFP antibodies (1:1000) overnight at 4 °C and then with Protein A resin for 1 h. The precipitate was washed with RIPA buffer three times. Finally, the resin was treated with SDS-PAGE loading buffer and boiled for 10 min. Western blotting was used to analyze the proteins with their correspondent antibodies.

TUNEL assay in HaEpi cells

The apoptosis was detected in HaEpi cells using the TUNEL Apoptosis kit (RIBOBIO, Guangzhou, China). The HaEpi cells were fixed within 4% paraformaldehyde for 15 min after treatment with 20E or an equal amount of DMSO for appropriate time. Then the cells were incubated with 0.5% Triton X-100 for 10 min at room temperature. After wash three times with PBS, 100 μL reaction mixtures covered cells and incubated for 2 h at 37 °C. The reaction was terminated by 200 μL 2×SSC (300 mM NaCl, 30 mM Na_3 citrate·$2H_2O$, pH 7.0) The nuclei were stained with 1 μg/mL 4', 6-diamidino-2-phenylindole (DAPI) for 10 min, and the resulting signals were observed using a Olympus FV3000 laser confocal microscope.

Statistical methods

Student's t test was used for the statistical analysis. The *p* value was calculated through paired and two tailed analysis (**p*<0.05, ***p*<0.01 and ****p*<0.001). The value indicated as the mean ± SD (standard deviation), n≥ 3. The density of the immunoreactive protein bands of the western blots was quantified using Quantity One software (Bio-Rad, Hercules, CA, USA). Three biological replicates and three technical replicates were performed for all experiments.

Acknowledgments

This work was supported by National Natural Science Foundation of China Grants 31730083 and 31572328. Shandong provincial key laboratory of animal cell and development biology, SPKLACDB-2019000. Thanks for the supports of startup fund from Northwest A&F University.

Author contributions

Cai-Hua Chen performed the major experiments and drafted the manuscript. Yu-Qin Di performed the hormone regulation on larvae. Qin-Yong Shen provided help on cell culture and materials preparation during experiments. Jin-Xing Wang and Xiao-Fan Zhao conceived studies

and edited the manuscript.

Conflict declaration

The authors declare no conflict of interest.

References

1. Parekh, A. B. (2010) Store-operated CRAC channels: function in health and disease. *Nat Rev Drug. Discov.* **9**, 399-410
2. Brini, M., and Carafoli, E. (2011) Calcium signaling and disease: preface. *BioFactors* **37**, 131
3. Clapham, D. E. (2007) Calcium signaling. *Cell* **131**, 1047-1058
4. Clapham, D. E. (1995) Calcium signaling. *Cell* **80**, 259-268
5. Stathopulos, P. B., Li, G. Y., Plevin, M. J., Ames, J. B., and Ikura, M. (2006) Stored Ca^{2+} depletion-induced oligomerization of stromal interaction molecule 1 (STIM1) via the EF-SAM region: An initiation mechanism for capacitive Ca^{2+} entry. *J. Biol. Chem.* **281**, 35855-35862
6. Liou, J., Kim, M. L., Heo, W. D., Jones, J. T., Myers, J. W., Ferrell, J. E., Jr., and Meyer, T. (2005) STIM is a Ca^{2+} sensor essential for Ca^{2+}-store-depletion-triggered Ca^{2+} influx. *Curr. biol.* **15**, 1235-1241
7. Roos, J., DiGregorio, P. J., Yeromin, A. V., Ohlsen, K., Lioudyno, M., Zhang, S., Safrina, O., Kozak, J. A., Wagner, S. L., Cahalan, M. D., Velicelebi, G., and Stauderman, K. A. (2005) STIM1, an essential and conserved component of store-operated Ca^{2+} channel function. *J. cell. biol.* **169**, 435-445
8. Nogueira, F. C., Silva, C. P., Alexandre, D., Samuels, R. I., Soares, E. L., Aragao, F. J., Palmisano, G., Domont, G. B., Roepstorff, P., and Campos, F. A. (2012) Global proteome changes in larvae of *Callosobruchus maculatus* Coleoptera:Chrysomelidae:Bruchinae) following ingestion of a cysteine proteinase inhibitor. *Proteomics* **12**, 2704-2715
9. Kobilka, B. K. (2007) G protein coupled receptor structure and activation. *Biochim. Biophys. Acta.* **1768**, 794-807
10. Luik, R. M., Wang, B., Prakriya, M., Wu, M. M., and Lewis, R. S. (2008) Oligomerization of STIM1 couples ER calcium depletion to CRAC channel activation. *Nature* **454**, 538-542
11. Gudlur, A., Zeraik, A. E., Hirve, N., Rajanikanth, V., Bobkov, A. A., Ma, G. L., Zheng, S. S., Wang, Y. J., Zhou, Y. B., Komives, E. A., and Hogan, P. G. (2018) Calcium sensing by the STIM1 ER-luminal domain. *Nat. Commun.* **9**
12. Liou, J., Fivaz, M., Inoue, T., and Meyer, T. (2007) Live-cell imaging reveals sequential oligomerization and local plasma membrane targeting of stromal interaction molecule 1 after Ca^{2+} store depletion. *Proc. Natl. Acad. Sci. U S A* **104**, 9301-9306
13. Yuan, J. P., Zeng, W., Dorwart, M. R., Choi, Y. J., Worley, P. F., and Muallem, S. (2009) SOAR and the polybasic STIM1 domains gate and regulate Orai channels. *Nat. cell biol.* **11**, 337-343
14. Feske, S., Gwack, Y., Prakriya, M., Srikanth, S., Puppel, S. H., Tanasa, B., Hogan, P. G., Lewis, R. S., Daly, M., and Rao, A. (2006) A mutation in Orai1 causes immune deficiency by abrogating CRAC channel function. *Nature* **441**, 179-185
15. Hogan, P. G., Lewis, R. S., and Rao, A. (2010) Molecular basis of calcium signaling in lymphocytes: STIM and ORAI. *Annu. Rev. Immunol.* **28**, 491-533
16. Hou, X., Pedi, L., Diver, M. M., and Long, S. B. (2012) Crystal structure of the calcium release-activated calcium channel Orai. *Science* **338**, 1308-1313
17. Balasuriya, D., Srivats, S., Murrell-Lagnado, R. D., and Edwardson, J. M. (2014) Atomic force microscopy (AFM) imaging suggests that stromal interaction molecule 1 (STIM1) binds to Orai1 with sixfold symmetry. *FEBS lett.* **588**, 2874-2880
18. Manji, S. S., Parker, N. J., Williams, R. T., van Stekelenburg, L., Pearson, R. B., Dziadek, M., and Smith, P. J. (2000) STIM1: a novel phosphoprotein located at the cell surface. *Biochim. Biophys. Acta.* **1481**, 147-155
19. Sheridan, J. T., Gilmore, R. C., Watson, M. J., Archer, C. B., and Tarran, R. (2013) 17beta-Estradiol inhibits phosphorylation of stromal interaction molecule 1 (STIM1) protein: implication for store-operated calcium entry and chronic lung diseases. *J. Biol. Chem.* **288**, 33509-33518
20. Smyth, J. T., Petranka, J. G., Boyles, R. R., DeHaven, W. I., Fukushima, M., Johnson, K. L., Williams, J. G., and Putney, J. W., Jr. (2009) Phosphorylation of STIM1 underlies suppression of store-operated calcium entry during mitosis. *Nat. cell biol.* **11**, 1465-1472
21. Pozo-Guisado, E., Casas-Rua, V., Tomas-Martin, P., Lopez-Guerrero, A. M., Alvarez-Barrientos, A., and Martin-Romero, F. J. (2013) Phosphorylation of STIM1 at ERK1/2 target sites regulates

interaction with the microtubule plus-end binding protein EB1. *J. Cell Sci.* **126**, 3170-3180
22. Heldring, N., Pike, A., Andersson, S., Matthews, J., Cheng, G., Hartman, J., Tujague, M., Strom, A., Treuter, E., Warner, M., and Gustafsson, J. A. (2007) Estrogen receptors: how do they signal and what are their targets. *Physiol. Rev.* **87**, 905-931
23. Thompson, E. B. (1995) Steroid hormones. Membrane transporters of steroid hormones. *Curr. Biol.* **5**, 730-732
24. Yang, D. L., Xu, J. W., Zhu, J. G., Zhang, Y. L., Xu, J. B., Sun, Q., Cao, X. N., Zuo, W. L., Xu, R. S., Huang, J. H., Jiang, F. N., Zhuo, Y. J., Xiao, B. Q., Liu, Y. Z., Yuan, D. B., Sun, Z. L., He, H. C., Lun, Z. R., Zhong, W. D., and Zhou, W. L. (2017) Role of GPR30 in estrogen-induced prostate epithelial apoptosis and benign prostatic hyperplasia. *Biochem. Biophys. Res. Commun.* **487**, 517-524
25. Manaboon, M., Iga, M., Iwami, M., and Sakurai, S. (2009) Intracellular mobilization of Ca^{2+} by the insect steroid hormone 20-hydroxyecdysone during programmed cell death in silkworm anterior silk glands. *J. Insect Physiol.* **55**, 122-128
26. Cai, M. J., Dong, D. J., Wang, Y., Liu, P. C., Liu, W., Wang, J. X., and Zhao, X. F. (2014) G-protein-coupled receptor participates in 20-hydroxyecdysone signaling on the plasma membrane. *Cell Commun. Signal.* **12**, 9
27. Wang, D., Zhao, W. L., Cai, M. J., Wang, J. X., and Zhao, X. F. (2015) G-protein-coupled receptor controls steroid hormone signaling in cell membrane. *Sci. Rep.* **5**, 8675
28. Liu, W., Cai, M. J., Wang, J. X., and Zhao, X. F. (2014) In a nongenomic action, steroid hormone 20-hydroxyecdysone induces phosphorylation of cyclin-dependent kinase 10 to promote gene transcription. *Endocrinology* **155**, 1738-1750
29. Liu, W., Cai, M. J., Zheng, C. C., Wang, J. X., and Zhao, X. F. (2014) Phospholipase Cgamma1 connects the cell membrane pathway to the nuclear receptor pathway in insect steroid hormone signaling. *J. Biol. Chem.* **289**, 13026-13041
30. Li, Y. B., Li, X. R., Yang, T., Wang, J. X., and Zhao, X. F. (2016) The steroid hormone 20-hydroxyecdysone promotes switching from autophagy to apoptosis by increasing intracellular calcium levels. *Insect Biochem. Mol. Biol.* **79**, 73-86
31. Jing, Y. P., Liu, W., Wang, J. X., and Zhao, X. F. (2015) The steroid hormone 20-hydroxyecdysone via nongenomic pathway activates Ca^{2+}/calmodulin-dependent protein kinase II to regulate gene expression. *J. Biol. Chem.* **290**, 8469-8481
32. Li, Y. B., Pei, X. Y., Wang, D., Chen, C. H., Cai, M. J., Wang, J. X., and Zhao, X. F. (2017) The steroid hormone 20-hydroxyecdysone upregulates calcium release-activated calcium channel modulator 1 expression to induce apoptosis in the midgut of *Helicoverpa armigera*. *Cell Calcium* **68**, 24-33
33. Thummel, C. S., and Chory, J. (2002) Steroid signaling in plants and insects--common themes, different pathways. *Genes Dev.* **16**, 3113-3129
34. Riddiford, L. M., Hiruma, K., Zhou, X., and Nelson, C. A. (2003) Insights into the molecular basis of the hormonal control of molting and metamorphosis from *Manduca sexta* and *Drosophila melanogaster*. *Insect Biochem. Mol. Biol.* **33**, 1327-1338
35. Chen, C. H., Pan, J., Di, Y. Q., Liu, W., Hou, L., Wang, J. X., and Zhao, X. F. (2017) Protein kinase C delta phosphorylates ecdysone receptor B1 to promote gene expression and apoptosis under 20-hydroxyecdysone regulation. *Proc. Natl. Acad. Sci. U S A* **114**, E7121-E7130
36. Wang, J. L., Jiang, X. J., Wang, Q., Hou, L. J., Xu, D. W., Wang, J. X., and Zhao, X. F. (2007) Identification and expression profile of a putative basement membrane protein gene in the midgut of *Helicoverpa armigera*. *BMC Dev. Biol.* **7**
37. Liu, C. Y., Liu, W., Zhao, W. L., Wang, J. X., and Zhao, X. F. (2013) Upregulation of the expression of prodeath serine/threonine protein kinase for programmed cell death by steroid hormone 20-hydroxyecdysone. *Apoptosis* **18**, 171-187
38. Muramatsu, Y., Maemoto, T., Iwashita, A., and Matsuoka, N. (2007) Novel neuroprotective compound SCH-20148 rescues thymocytes and SH-SY5Y cells from thapsigargin-induced mitochondrial membrane potential reduction and cell death. *Eur. J. Pharmacol.* **563**, 40-48
39. Chung, W. C., and Kermode, J. C. (2005) Suramin disrupts receptor-G protein coupling by blocking association of G protein alpha and betagamma subunits. *J. Pharmacol. Exp. Ther.* **313**, 191-198

40. Yule, D. I., and Williams, J. A. (1992) U73122 inhibits Ca^{2+} oscillations in response to cholecystokinin and carbachol but not to JMV-180 in rat pancreatic acinar cells. *J. Biol. Chem.* **267**, 13830-13835
41. De Smet, P., Parys, J. B., Callewaert, G., Weidema, A. F., Hill, E., De Smedt, H., Erneux, C., Sorrentino, V., and Missiaen, L. (1999) Xestospongin C is an equally potent inhibitor of the inositol 1,4,5-trisphosphate receptor and the endoplasmic-reticulum $Ca^{(2+)}$ pumps. *Cell Calcium* **26**, 9-13
42. Chmura, S. J., Dolan, M. E., Cha, A., Mauceri, H. J., Kufe, D. W., and Weichselbaum, R. R. (2000) In vitro and in vivo activity of protein kinase C inhibitor chelerythrine chloride induces tumor cell toxicity and growth delay in vivo. *Clin. Cancer Res.* **6**, 737-742
43. Wang, D., Pei, X. Y., Zhao, W. L., and Zhao, X. F. (2016) Steroid hormone 20-hydroxyecdysone promotes higher calcium mobilization to induce apoptosis. *Cell Calcium* **60**, 1-12
44. Zhou, Y., Srinivasan, P., Razavi, S., Seymour, S., Meraner, P., Gudlur, A., Stathopulos, P. B., Ikura, M., Rao, A., and Hogan, P. G. (2013) Initial activation of STIM1, the regulator of store-operated calcium entry. *Nat. Struct. Mol. Biol.* **20**, 973-981
45. Berry, P. A., Birnie, R., Droop, A. P., Maitland, N. J., and Collins, A. T. (2011) The calcium sensor STIM1 is regulated by androgens in prostate stromal cells. *Prostate* **71**, 1646-1655
46. Eylenstein, A., Schmidt, S., Gu, S., Yang, W., Schmid, E., Schmidt, E. M., Alesutan, I., Szteyn, K., Regel, I., Shumilina, E., and Lang, F. (2012) Transcription factor NF-kappaB regulates expression of pore-forming Ca^{2+} channel unit, Orai1, and its activator, STIM1, to control Ca^{2+} entry and affect cellular functions. *J. Biol. Chem.* **287**, 2719-2730
47. Eylenstein, A., Gehring, E. M., Heise, N., Shumilina, E., Schmidt, S., Szteyn, K., Munzer, P., Nurbaeva, M. K., Eichenmuller, M., Tyan, L., Regel, I., Foller, M., Kuhl, D., Soboloff, J., Penner, R., and Lang, F. (2011) Stimulation of Ca^{2+}-channel Orai1/STIM1 by serum- and glucocorticoid-inducible kinase 1 (SGK1). *FASEB J* **25**, 2012-2021
48. Jing, Y. P., Wang, D., Han, X. L., Dong, D. J., Wang, J. X., and Zhao, X. F. (2016) The Steroid Hormone 20-Hydroxyecdysone Enhances Gene Transcription through the cAMP Response Element-binding Protein (CREB) Signaling Pathway. *J. Biol. Chem.* **291**, 12771-12785
49. Palli, S. R., Hiruma, K., and Riddiford, L. M. (1992) An ecdysteroid-inducible *Manduca* gene similar to the *Drosophila* DHR3 gene, a member of the steroid hormone receptor superfamily. *Dev. Biol.* **150**, 306-318
50. Lan, Q., Hiruma, K., Hu, X., Jindra, M., and Riddiford, L. M. (1999) Activation of a delayed-early gene encoding MHR3 by the ecdysone receptor heterodimer EcR-B1-USP-1 but not by EcR-B1-USP-2. *Mol. Cell. Biol.* **19**, 4897-4906
51. Liu, P. C., Wang, J. X., Song, Q. S., and Zhao, X. F. (2011) The participation of calponin in the cross talk between 20-hydroxyecdysone and juvenile hormone signaling pathways by phosphorylation variation. *Plos One* **6**, e19776
52. Soboloff, J., Madesh, M., and Gill, D. L. (2011) Sensing cellular stress through STIM proteins. *Nat. Chem. Biol.* **7**, 488-492
53. Melien, O., Nilssen, L. S., Dajani, O. F., Sand, K. L., Iversen, J. G., Sandnes, D. L., and Christoffersen, T. (2002) Ca^{2+}-mediated activation of ERK in hepatocytes by norepinephrine and prostaglandin F2 alpha: role of calmodulin and Src kinases. *BMC Cell Biol.* **3**, 5
54. Eid, J. P., Arias, A. M., Robertson, H., Hime, G. R., and Dziadek, M. (2008) The *Drosophila* STIM1 orthologue, dSTIM, has roles in cell fate specification and tissue patterning. *BMC Dev. Biol.* **8**, 104
55. Zhao, X. F., Wang, J. X., and Wang, Y. X. (1998) Purification and characterization of a cysteine proteinase from eggs of the cotton boll worm, *Helicoverpa armigera*. *Insect Biochem Mol Biol* **28**, 259-264
56. Shao, H. L., Zheng, W. W., Liu, P. C., Wang, Q., Wang, J. X., and Zhao, X. F. (2008) Establishment of a new cell line from lepidopteran epidermis and hormonal regulation on the genes. *Plos One* **3**
57. Liu, W., Zhang, F. X., Cai, M. J., Zhao, W. L., Li, X. R., Wang, J. X., and Zhao, X. F. (2013) The hormone-dependent function of Hsp90 in the crosstalk between 20-hydroxyecdysone and juvenile hormone signaling pathways in insects is determined by differential phosphorylation and protein interactions. *Biochim. Biophys. Acta*. **1830**, 5184-5192

58. Bradford, M. M. (1976) A rapid and sensitive method for the quantitation of microgram quantities of protein utilizing the principle of protein-dye binding. *Anal. Biochem.* **72**, 248-254
59. Fire, A., Xu, S., Montgomery, M. K., Kostas, S. A., Driver, S. E., and Mello, C. C. (1998) Potent and specific genetic interference by double-stranded RNA in *Caenorhabditis elegans*. *Nature* **391**, 806-811
60. Zamore, P. D., Tuschl, T., Sharp, P. A., and Bartel, D. P. (2000) RNAi: double-stranded RNA directs the ATP-dependent cleavage of mRNA at 21 to 23 nucleotide intervals. *Cell* **101**, 25-33
61. Terenius, O., Papanicolaou, A., Garbutt, J. S., Eleftherianos, I., Huvenne, H., Kanginakudru, S., Albrechtsen, M., An, C., Aymeric, J. L., Barthel, A., Bebas, P., Bitra, K., Bravo, A., Chevalier, F., Collinge, D. P., Crava, C. M., de Maagd, R. A., Duvic, B., Erlandson, M., Faye, I., Felfoldi, G., Fujiwara, H., Futahashi, R., Gandhe, A. S., Gatehouse, H. S., Gatehouse, L. N., Giebultowicz, J. M., Gomez, I., Grimmelikhuijzen, C. J., Groot, A. T., Hauser, F., Heckel, D. G., Hegedus, D. D., Hrycaj, S., Huang, L., Hull, J. J., Iatrou, K., Iga, M., Kanost, M. R., Kotwica, J., Li, C., Li, J., Liu, J., Lundmark, M., Matsumoto, S., Meyering-Vos, M., Millichap, P. J., Monteiro, A., Mrinal, N., Niimi, T., Nowara, D., Ohnishi, A., Oostra, V., Ozaki, K., Papakonstantinou, M., Popadic, A., Rajam, M. V., Saenko, S., Simpson, R. M., Soberon, M., Strand, M. R., Tomita, S., Toprak, U., Wang, P., Wee, C. W., Whyard, S., Zhang, W., Nagaraju, J., Ffrench-Constant, R. H., Herrero, S., Gordon, K., Swevers, L., and Smagghe, G. (2011) RNA interference in Lepidoptera: an overview of successful and unsuccessful studies and implications for experimental design. *J. Insect Pphysiol.* **57**, 231-245
62. Livak, K. J., and Schmittgen, T. D. (2001) Analysis of relative gene expression data using real-time quantitative PCR and the 2(-Delta Delta C(T)) Method. *Methods* **25**, 402-408
63. Hou, L., Wang, J. X., and Zhao, X. F. (2011) Rab32 and the remodeling of the imaginal midgut in *Helicoverpa armigera*. *Amino Acids* **40**, 953-961

Table 1. The predicted EcRE sequences in STIM1 promoters from different species

Species	Sequence (5'-3')
Helicoverpa armigera	$_{-34}$ g c g g T t A a T G c A t T a $_{-20}$
Bombyx mori	$_{-34}$ g c g g T t A g T G c A t T a $_{-20}$
Drosophila melanogaster	$_{-931}$g a a t T c A t T G t A t T t$_{-917}$
Plutella xylostella	$_{-736}$a a g g T c A t T t c A c T t$_{-722}$
Apis florea	$_{-833}$a a a t T t A a T G a t a T t$_{-819}$

Table 2. Oligonucleotide sequences of PCR primers

Primer name	Sequence (5'-3')
qRT-PCR	
STIM1-RT F	ggtgacacgccgctactg
STIM1-RT R	tcttccaactcgccctcc
EcRB1-RT F	aattgcccgtcagtacga
EcRB1-RT R	tgagcttctcattgagga
USP1-RT F	ggtcctgacagcaatgtt
USP1-RT R	ttccagctccagctgactgaag
HR3-RT F	tcaagcacctcaacagcagcccta
HR3-RT R	gactttgctgatgtcaccctccgc
BrZ7-RT F	ggtgactgtccttactgcggcat
BrZ7-RT R	ttaattcctttgaccatgact
caspase-3 RT F	ggagacaagggtggagaa
caspase-3 RT R	ggaaggcgtgtatgtggt
caspase-6 RT F	gctgtgatcagtgctacggat
caspase-6 RT R	ccgaatcagctgcatacactt
RPL27-RT F	acaggtatccccgcaaagtgc
RPL27-RT R	gtccttggcgctgaacttctc
β-actin RT F	cctggtattgctgaccgtatgc
β-actin RT R	ctgttggaaggtggagagggaa
ChIP assay	
EcRE F	cattgaacttgtgatgtggc
EcRE R	cgtgatctcacaatgacac
RNA interference:	
STIM1RNAi F	gcgtaatacgactcactatagggagaatattggtgcgtatttgct
STIM1RNAi R	gcgtaatacgactcactatagggagatttgtggatagggtctttg
EcRB1RNAi F	gcgtaatacgactcactatagggacgctggtataacaacggagga
EcRB1RNAi R	gcgtaatacgactcactatagggaagctggagacaactcctcacg
USP1RNAi F	gcgtaatacgactcactatagggacgaaccatcccctaagtggttc
USP1RNAi R	gcgtaatacgactcactatagggaccttgatgagcaggatctggtc
ErGPCR-1 RNAi F	gcgtaatacgactcactatagggttcatccttctaacggtggc
ErGPCR-1 RNAi R	gcgtaatacgactcactatagggtcgcttcatcttcgctatct
ErGPCR-2 RNAi F	gcgtaatacgactcactataggcgagggtcaagtctgaggtt
ErGPCR-2 RNAi R	gcgtaatacgactcactataggttaaggctgtttgatgttga
GFPRNAi F	gcgtaatacgactcactatagggatggtcccaattctcgtggaac
GFPRNAi R	gcgtaatacgactcactatagggacttgaagttgaccttgatgcc
Overexpression:	
STIM1oex F	caggagatctcgatgcgtatcggtttcgtg
STIM1oex R	taatacggtacccttatcccctcctaatataaag
EcRB1oex F	taacacgtcaagagctcatgagacgccgctggtataac
EcRB1oex R	gcaggcgcgccgagatctggagcgccggcgagtccgcca

Figures and Figure legends

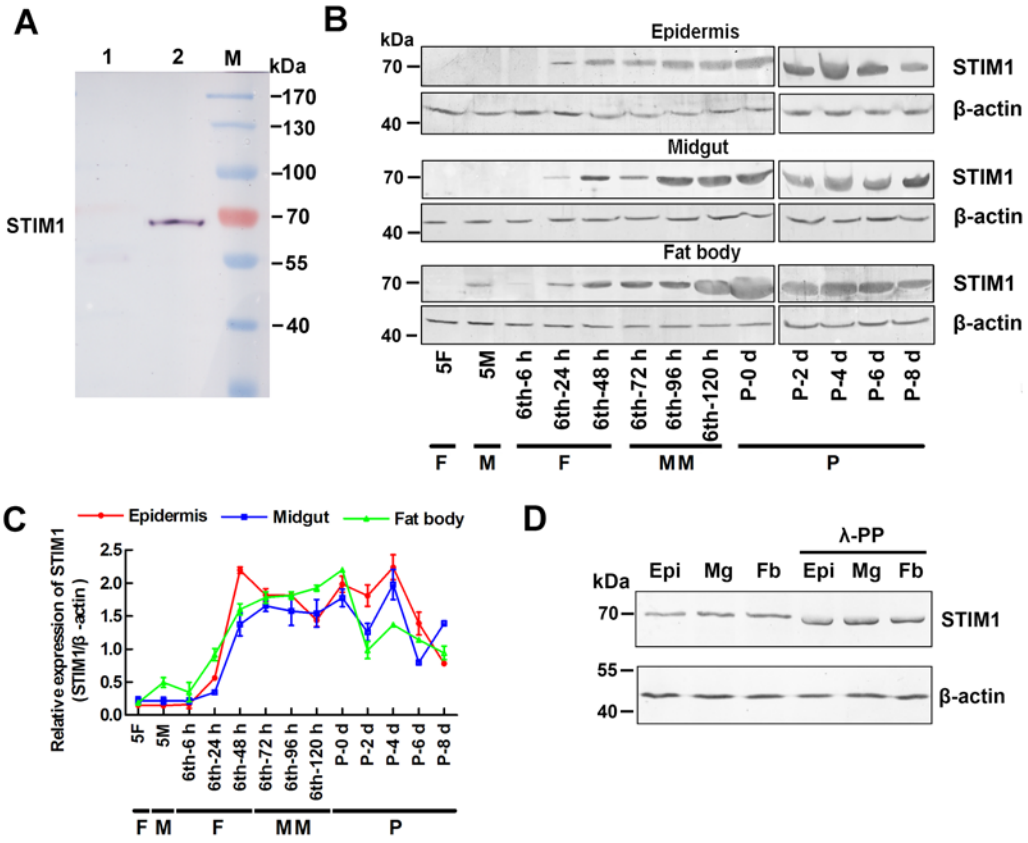

Figure 1. Western blot analysis of the expression and phosphorylation of STIM1 in different tissues during development. ***(A)*** Examination of the specificity of the polyclonal antibodies against *H. armigera* STIM1 by western blot. M: Maker; Line 1: pre-serum; Line 2: anti-serum. The proteins were from the midgut of sixth instar 72 h larvae. Anti-rabbit IgG (AP) was used as the secondary antibody. ***(B)*** Expression profiles of STIM1 in the epidermis, midgut, and fat body were detected using anti-STIM1 antibodies. β-actin was used as the protein quantity control. **5F**, fifth instar feeding larvae; **5M**, fifth instar molting larvae; **6th-6 h** to **6th-120 h** represent sixth instar larvae at the corresponding hours. **P-0 d** to **P-8 d** indicate 0- to 8-d-old pupae. **F**, feeding; **M**, molting; **MM**, metamorphic molting; **P**, pupae. The molecular weight markers were indicated on the left. ***(C)*** The immunoreactive protein bands were subjected to densitometry analyses using Quantity One software based on three independent biological experiments. The bars indicate the means ± SD of three independent experiments. ***(D)*** Examination of STIM1 phosphorylation. The λ phosphatase (λ-PP) treated proteins extracted from epidermis, midgut, and fat body of 6th-72 h larvae. The gel concentrations were 7.5% for all experiments. The left numbers means the molecular weight markers.

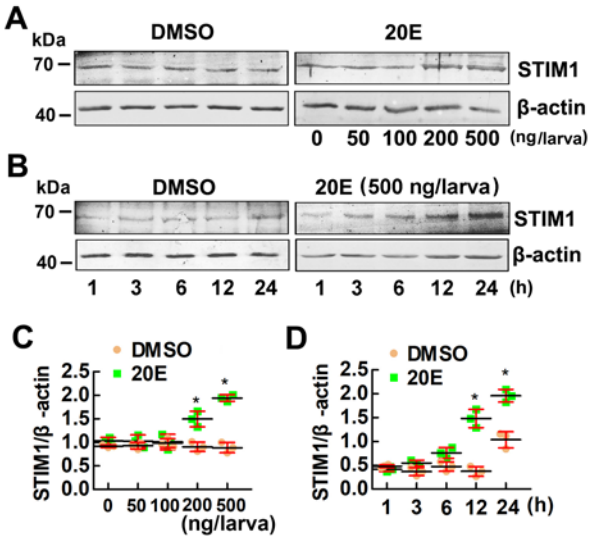

Figure 2. Western blotting showed the upregulated level of STIM1 by 20E in the midgut. (*A*) 20E was injected into larvae at the 6th instar 6 h (6th-6 h larvae) at different concentrations for 24 h. An equal amount of diluted DMSO was injected as the control. β-actin was detected as the protein quantity control. ***(B)*** Injection of 500 ng of 20E per 6th-6 h larva for different times. DMSO was used as the solvent control and β-actin as the protein quality control. All gel concentrations were 7.5%. The molecular weight markers near the bands were indicated. ***(C)*** and ***(D)*** The immunoreactive protein bands in ***A*** and ***B*** were subjected to densitometry analyses using Quantity One software. The bars indicate the mean ± SD. Significant differences were calculated using Student's t test (*$p < 0.05$) based on three biological replicates.

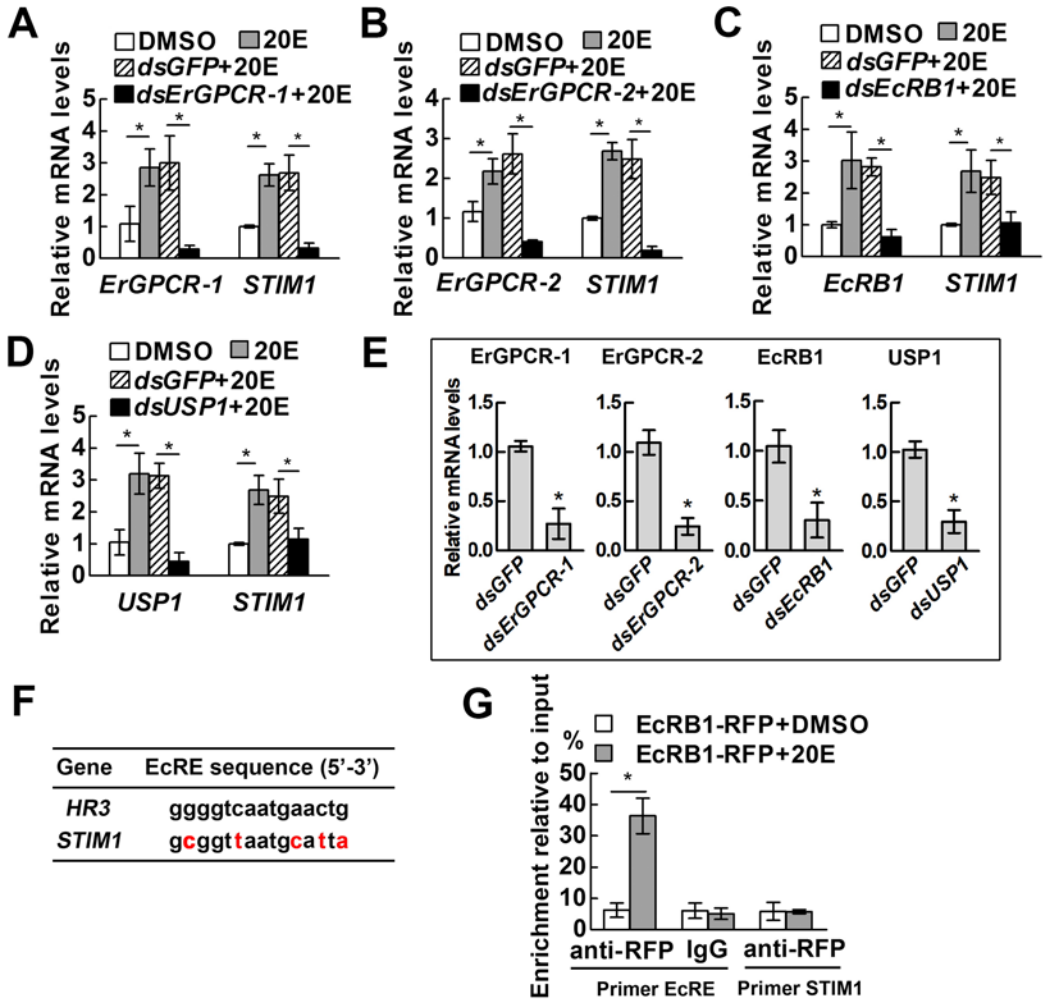

Figure 3. 20E promotes *STIM1* transcription through GPCRs, EcRB1, and USP1. Knockdown *ErGPCR-1* ***(A)***, *ErGPCR-2* ***(B)***, *EcRB1* ***(C)*** and *USP1* ***(D)*** using RNAi in HaEpi cells and detection of the transcript of *STIM1* using qRT-PCR after treatment with 20E (2 μM) for 12 h. The relative mRNA levels were calculated using the $2^{-\Delta\Delta Ct}$ method as described in the methods. ***(E)*** The interference efficiencies of the four genes were detected separately by qRT-PCR. The bars indicate the means ± SD of three independent experiments. ***(F)*** The EcRE sequence was predicted in the *HR3* and *STIM1* promoter regions in *H. armigera*. ***(G)*** Detection of EcRB1 binding to EcRE to increase *STIM1* transcription via a ChIP assay. EcRB1-RFP was overexpressed in HaEpi cells for 72 h. The cells were treated with 20E (2 μM) or an equal amount of DMSO for 12 h. ChIP assays were quantified using qRT-PCR with the DNA template in the precipitates and an antibody against RFP. Enrichment relative to input = (sample precipitated by antibody – sample without antibody)/input × %. **Input**, sample before immunoprecipitation. **lgG**, nonspecific mouse lgG. **Primer EcRE**, primers targeting the EcRE. **Primer STIM1**, primers targeted to the *STIM1* ORF. Statistical analyses were performed using Student's t test (*$p < 0.05$), and the values are the mean ± SD. Three biological replicates and three technical replicates were performed for all experiments.

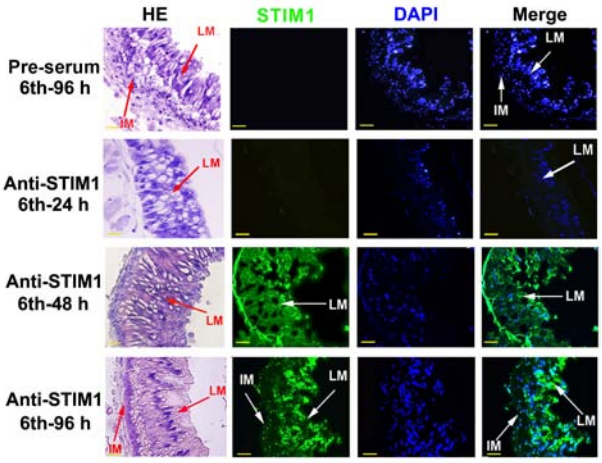

Figure 4. STIM1 is located in the larval midgut during metamorphosis. Hematoxylin and eosin (HE) staining showing the tissue histology of the midgut at different developmental stages. Immunohistochemistry was used to identify the location of STIM1. **IM**, imaginal midgut; **LM**, larval midgut. The green fluorescence indicates STIM1 detected using an anti-STIM1 antibody. The blue fluorescence indicates the nuclei stained with DAPI. Rabbit pre-serum was used as a control for the antibody. The yellow bar =50 μm.

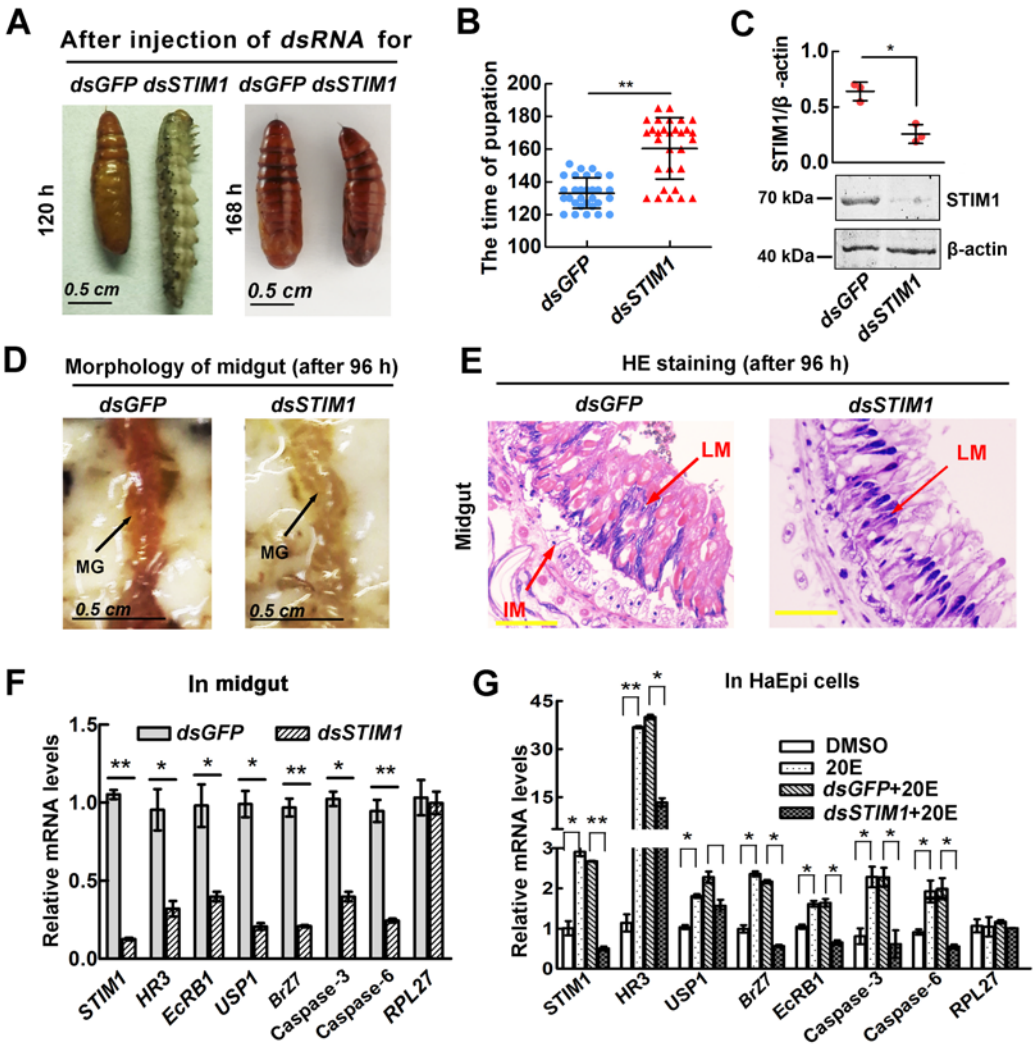

Figure 5. *STIM1* knockdown delayed larval-pupal transition and decreased 20E-responsive gene expression. ***(A)*** Phenotypes of larvae and pupae after injection of *dsSTIM1* and *dsGFP* (negative control). *dsRNA* (1 μg and 2 μg*)* was injected into fifth instar 12 h and sixth instar 6 h larvae, respectively. ***(B)*** Statistical analysis of the time of pupation after injection *dsGFP* or *dsSTIM1*. Each group contained 30 larvae. The values are the means ± SD. The significant differences were determined using Student's t test (***p <0.001) based on three repeats. ***(C)*** Western blotting showing the efficiency of *STIM1* knockdown. Proteins of the midgut were extracted from 96 h-injected larvae. The gel concentration was 7.5%. β-actin was used as the loading control. The immunoreactive protein bands were subjected to densitometry analyses using Quantity One software. The values are the means ± SD (n = 3). The significant differences were determined using Student's t test (*p < 0.05). ***(D)*** Morphology of midgut after a second injection of *dsRNA* for 96 h. **MG**: midgut. ***(E)*** HE staining showing the tissue histology of the midgut after the second injection of *dsGFP* or *dsSTIM1* for 96 h. Scale bar = 50 μm. ***(F)*** and ***(G)*** Relative mRNA levels of 20E-induced genes in the larval midgut and in HaEpi cells after knockdown of *STIM1*. *dsGFP* was the negative control. Total mRNA isolated from larval midgut after the second injection for 96 h for qRT-PCR analysis, and from HaEpi cells transfected with *dsSTIM1* or *dsGFP* for 24 h and subsequently treated with 20E (2 μM) for 12 h. An equal volume of DMSO was used as the control. The relative mRNA levels were determined using the $2^{-\Delta\Delta CT}$ method. *RPL27* was included as a non-specific target control of the RNAi. The bars indicate the

means ± SD of three independent biological experiments. The asterisks denote significant differences, as determined using Student's t test (* $p < 0.05$; ** $p < 0.01$).

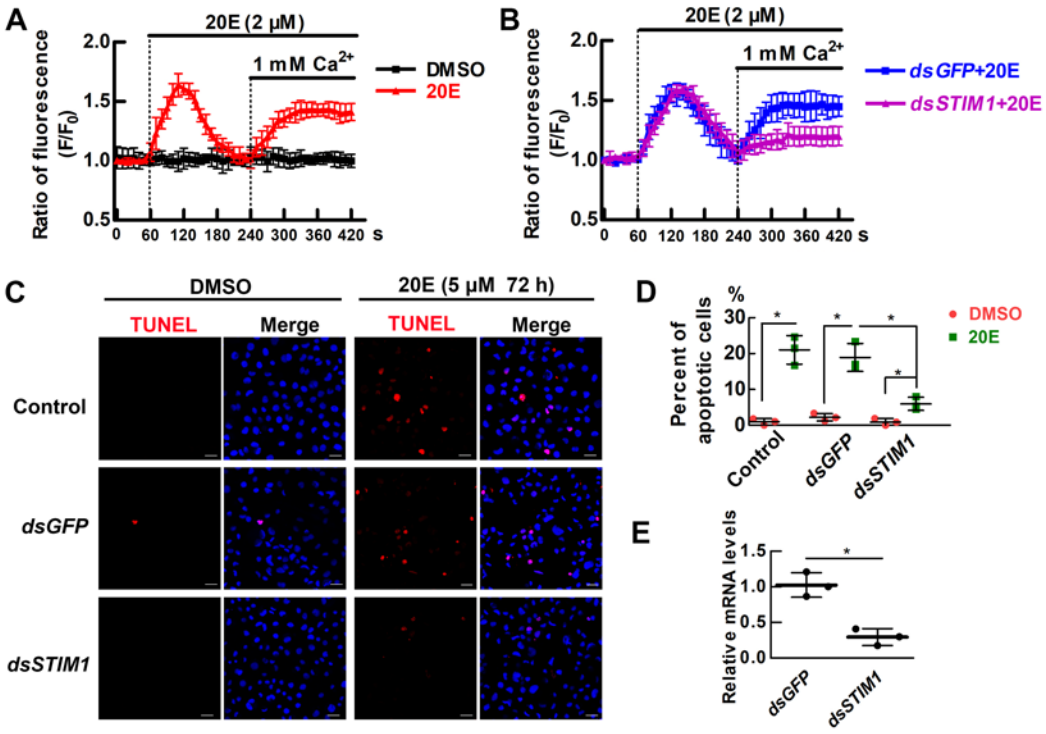

Figure 6. Knockdown of *STIM1* inhibited 20E-induced Ca^{2+} influx. ***(A)*** 20E increased cytosolic Ca^{2+} levels. The first peak is the intracellular Ca^{2+} release from the intracellular store induced by 2 μM 20E for 2 min. The second peak is the Ca^{2+} influx induced by the addition of 1 mM $CaCl_2$ into the medium. **F:** the fluorescence of the AM ester Calcium Crimson™ dye indicating the free calcium in cells. **F0:** The fluorescence of resting cells. The bars indicate the means ± SD of three independent biological experiments. ***(B)*** Knockdown of *STIM1* repressed 20E-induced Ca^{2+} influx. The cytosolic Ca^{2+} levels were detected after cells were transfected with *dsSTIM1* or *dsGFP* (negative control) for 48 h. ***(C)*** The apoptotic cells were examined by TUNEL experiments after 20E or DMSO induction. The red signal means the apoptotic cells. The blue fluorescence indicates the nuclei stained with DAPI. The bar = 20 μm. ***(D)*** Statistical analysis of the ratio of apoptotic cells. The significant differences were determined using Student's *t* test from three biological repeats (*p < 0.05). The values are the mean ± SD. ***(E)*** qRT-PCR detected the efficiency of *STIM1* knockdown in cells. mRNA was isolated after cells were transfected with *dsSTIM1* or *dsGFP* for 48 h. The bars indicate the means ± SD of three independent biological experiments. The significant differences were determined using Student's t test (* $p < 0.05$).

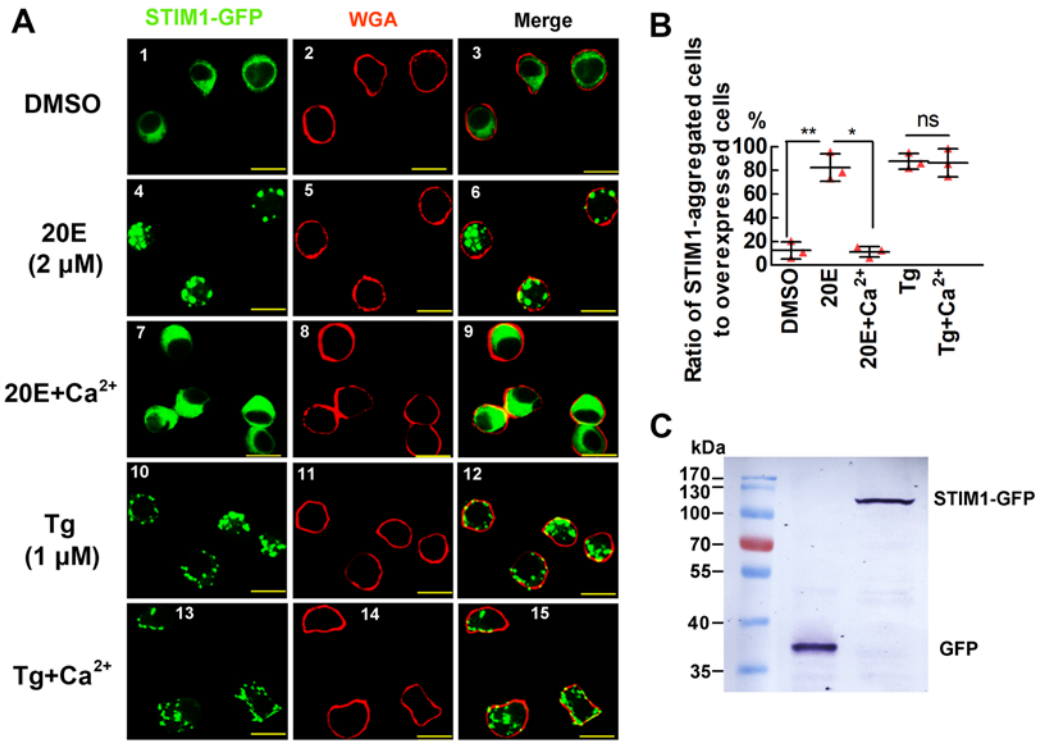

Figure 7. 20E induced translocation of STIM1-GFP toward the PM, which clustered into puncta underneath the PM in HaEpi cells. ***(A)***Panels 1-6 and 10-12 show cells treated with DMSO, 20E, or Tg for 10 min in DPBS. Panels 7-9 and 13-15 show cells treated with 20E or Tg for 10 min in DPBS, followed 1 mM Ca^{2+} incubation for another 10 min. The red fluorescence indicates the plasma membrane stained with Alexa Fluor 594-conjugated wheat germ agglutinin (WGA). The bars denote 20 μm. ***(B)*** Statistical analysis of the ratio of STIM1-aggregated cells among the overexpressing cells. The significant differences were determined using Student's *t* test from three biological repeats (*$p < 0.05$; **$p < 0.01$). The values are the mean ± SD. ***(C)*** western bolt showed the GFP and STIM1-GFP in HaEpi cells. The gel concentration was 7.5%.

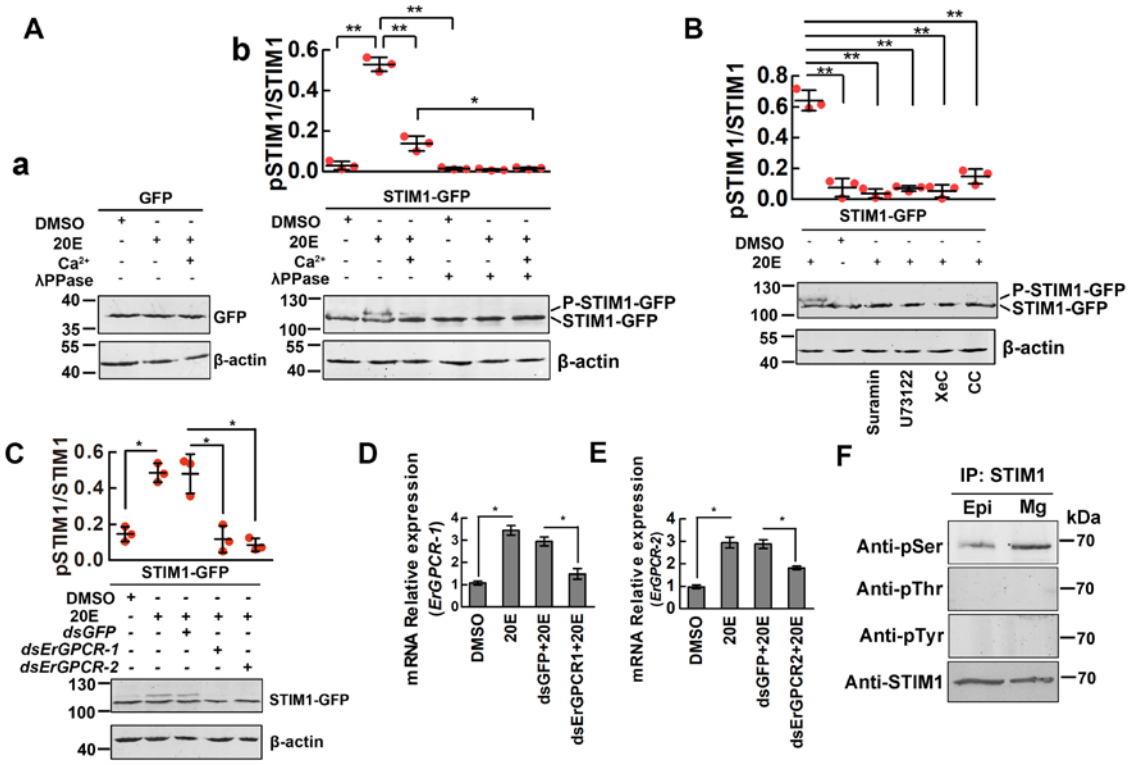

Figure 8. STIM1 phosphorylation was induced by 20E via the GPCR-, PLC-, IP3R- and PKC- signal axis. ***(A)*** Western blotting analysis of the phosphorylation of STIM1 in HaEpi cells. STIM1-GFP and GFP were overexpressed in HaEpi cells for 48 hours. The cells were treated with 20E (2 μM) or an equal volume of DMSO as a solvent control for 10 min in Ca^{2+} free DPBS. Thereafter, the cells were incubated Ca^{2+}-containing DPBS (1 mM) for 10 min. A portion of the protein extract was treated with λ-phosphatase. ***(a)*** GFP-tag as a control after induction of DMSO or 20E. ***(b)*** 20E induced phosphorylation of STIM1. Mouse GFP monoclonal antibody was used to detect STIM1-GFP. Anti-mouse IgG (AP) was used as the secondary antibody. The immunoreactive protein bands were subjected to densitometry analyses using Quantity One software based on three independent biological experiments. The molecular weight markers (kDa) were indicated for all blot. ***(B)*** 20E-induced phosphorylation of STIM1 was suppressed by the GPCR inhibitor Suramin (50 μM), the PLC inhibitor U73122 (10 μM), the IP_3R inhibitor Xestospongin (XeC) (3 μM), and the PKC inhibitor Chelerythrine Chloride (CC) (5 μM). Western blotting and statistical analyses were performed as in (*A*). ***(C)*** Knockdown of *ErGPCR-1* and *ErGPCR-2* in HaEpi cells using RNAi repressed 20E-induced STIM1 phosphorylation. The *dsRNA*-treated cells were incubated with 20E (2 μM) or DMSO for 10 min in DPBS without Ca^{2+}. ***(D)*** and ***(E)*** Efficacy of RNAi of *ErGPCR1* and *ErGPCR2*. After the cells were transfected with dsRNA for 48 h and then treated with 2 μM 20E or DMSO for 12 h, the total RNA were extracted for qRT-PCR. For A-E, the significant differences were determined using Student's t test (* $p < 0.05$; **$p < 0.01$). Values are the mean ± SD from three independent experiments. ***(F)*** The phosphorylation residue type of STIM1 in tissues. STIM1 was precipitated from the epidermis and midgut of sixth instar 72 h larvae using anti-STIM1 polyclonal antibodies. Antibodies recognizing pSer, pThr and pTyr were used as described in the methods. All the gel concentrations used in western blotting were 7.5%.

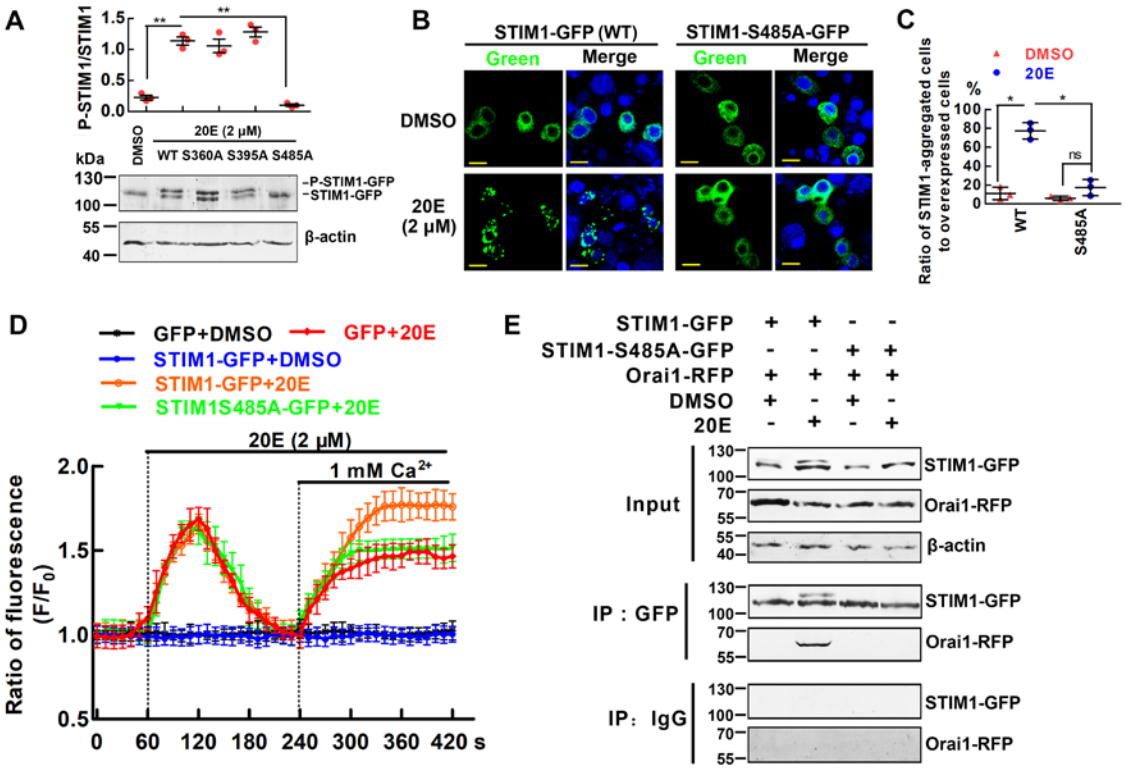

Figure 9. Identification of the STIM1 phosphorylation site and its functions. ***(A)*** Western blot showing the MW of the STIM1-GFP-His and its site mutants (S360A, S395A, and S485A). STIM1-GFP-His and three single site mutants were overexpressed in HaEpi cells for 48 h. The cells were then treated with 20E (2 μM) for 15 min in Ca^{2+} free DPBS. β-actin was used as a loading control. The gel concentration was 7.5%. The left numbers showed the molecular weight markers. The immunoreactive protein bands were subjected to densitometry analyses using Quantity One software. Values are means ± SD from three independent experiments. The significant differences were determined using Student's t test (** $p< 0.01$). ***(B)*** Detection the aggregation of STIM1 and its mutant (S485A) under 20E induction. Cells were treated with 20E (2 μM) in DPBS for 15 min after STIM1-GFP and STIM1-S485A-GFP were overexpressed. The nuclei were mstained with DAPI. The yellow bar = 20 μm. ***(C)*** Statistical analysis of the ratio of STIM1-aggregated cells among the overexpressing cells. The significant differences were determined using Student's *t* test from three biological repeats (*$p < 0.05$). ***(D)*** The cytosolic Ca^{2+} levels induced by STIM1-GFP and STIM1-S485A mutant overexpression in HaEpi cells. 20E (2 μM) and 1 Ca^{2+} mM were added to the cells at the corresponding times. The Ca^{2+} curves represented three biological replicates. Values are means ± SD. ***(E)*** Co-IP detected the interaction of STIM1 (wild-type and S485A mutant) and Orai1. STIM1-GFP or STIM1-S485A-GFP and Orai1-RFP were co-transfected into HaEpi cells. After 72 h, the cells were treated with 2 μM 20E or DMSO for 15 min in DPBS without Ca^{2+}. The proteins were extracted for Co-IP as described in the methods. IgG means a nonspecific antibody as a negative control. The gel concentrations for western blotting were 7.5%. Three biological replicates and three technical replicates were performed for the experiment.

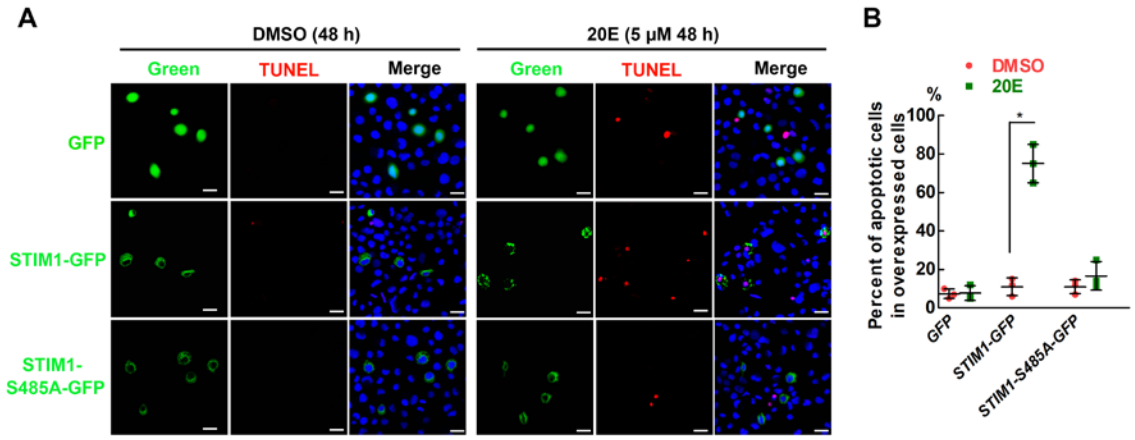

Figure 10. Detection of apoptosis in STIM1-RFP and STIM1-S485A-RFP overexpressing cells after 20E induction. ***(A)*** Cells were transfected using the three plasmids for 48 h and then treated with 5 μM 20E or an equal amount of DMSO for 48 h. The cell apoptosis were detected by TUNEL assay. The nuclei were stained with DAPI. Red fluorescence indicated apoptotic cells. Th e bar = 20 μm. ***(B)*** Statistical analysis of the proportion of apoptotic cells among the overexpressing cells. The significant differences were determined using Student's *t* test from three biological repeats (*$p < 0.01$). The values are the mean ± SD.

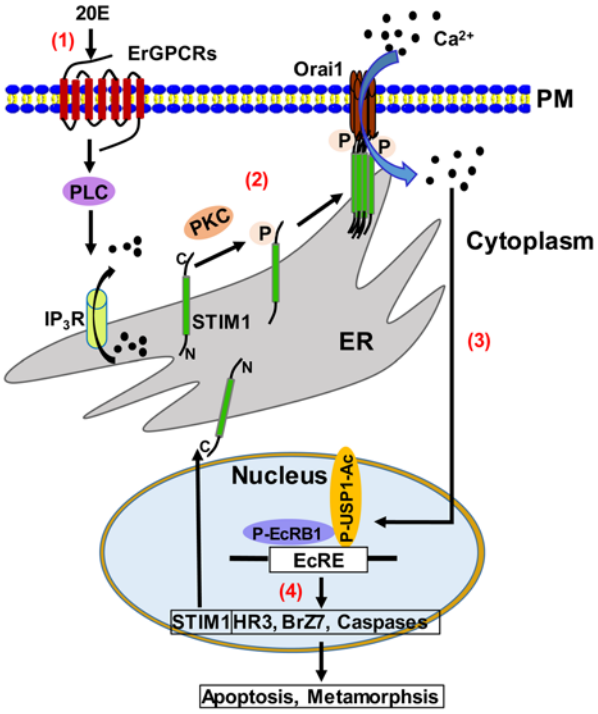

Figure 11. Schematic diagram showing the mechanism of STIM1 in insect development under 20E induction. (1) 20E, through ErGPCRs-, PLC- and IP_3R- signal pathways, rapidly induces calcium release from ER into the cytoplasm. **(2)** PKC promotes STIM1 phosphorylation at Ser485, causing STIM1 aggregation. The aggregated-STIM1 moves toward the PM and interacts with Orai1 on the PM to induce calcium influx in a few minutes. **(3)** The increased calcium triggers P-EcRB1/P-USP1-Ac transcriptional complex formation. **(4)** EcRB1 and USP1 bind to EcRE to upregulate transcription of *STIM1* and other genes in 20E pathway in a longer time. STIM1 participates in 20E-induced SOCE in a positive feedback manner. Via SOCE, 20E induces apoptosis in the midgut during metamorphosis.

The steroid hormone 20-hydroxyecdysone induces phosphorylation and aggregation of stromal interacting molecule 1 for store-operated calcium entry

Cai-Hua Chen, Yu-Qin Di, Qin-Yong Shen, Jin-Xing Wang and Xiao-Fan Zhao

J. Biol. Chem. published online August 14, 2019
